

# Characteristic Analysis of Superheater Tubes of Biomass Direct-fired Boilers

Hao Zhou

Jiangsu Vocational College of Business, Nantong 226011, China  
[zhouhao2008364@163.com](mailto:zhouhao2008364@163.com)

This paper studies the characteristics of superheater tubes in biomass direct-fired boilers through corrosive thinning and kinetic analysis, corrosion product analysis and the effect of HCl concentration. The experimental results show that the corrosion resistance of TC4 tube materials is good; the corrosion resistance of pure titanium tube is relatively poorer compared with the former; the tube with higher nickel content have better corrosion resistance. Therefore, in the selection of materials for superheater tubes of biomass direct-fired boilers, it is necessary to select tubes with higher nickel content to prolong the service life of superheaters.

## 1. Introduction

With the development of science and technology, biomass direct-fired boilers are widely used in China's power industry, but the problem of poor corrosion resistance of superheater tubes of biomass direct-fired boilers has always existed. Based on this, the characteristic analysis of superheater tubes of biomass direct-fired boilers is of great significance to reduce the corrosion of superheater tubes.

## 2. Literature review

Superheater tubes in biomass-fired power plants experience high corrosion rates due to condensation of corrosive alkali chloride-rich deposits (Okoro et al., 2016). The tube burst is related to the ash of biomass fuel and many short-terms over-high temperature. Wood pellets were not problematic for about ten years, contrary to a mixture of demolition wood, wood cuttings, compost overflow, paper sludge and roadside grass which caused excessive fouling at a superheater bundle after already a few weeks (Stam et al., 2014). Superheater tubes of biomass-fired boilers at considerably higher temperatures than can be tolerated by commonly used structural materials could improve boiler efficiency. However, corrosion of the superheater tubes promoted by interaction with the relatively low melting point deposits that accumulate on the tubes becomes a major issue. Corrosion probes containing multiple specimens of nine different alloys were exposed for at least 2000 h in the superheater area of three biomass boilers where the deposits were determined to be enriched in potassium or chlorine. Similar specimens were also exposed in a boiler co-firing coal and wood (Kerser et al., 2014). Most biomass fuels have a high content of alkali metals and chlorine, but they contain very little sulphur compared to fossil fuels. Potassium chloride, KCl, is found in the gas phase, condenses on the superheater tubes and forms complex alkali salts with iron and other elements in the steels. These salts have low melting points and are very corrosive. The corrosion can be mitigated by use of an instrument for in-situ measurement of alkali chlorides in the flue gases, in combination with the addition of ammonium sulphate. An ammonium sulphate solution, specially developed for the reduction of corrosion was sprayed into the flue gases and effectively converted KCl into potassium sulphate, K<sub>2</sub>SO<sub>4</sub>, much less corrosive than KCl. Deposit probe tests and long-term corrosion probe tests have been performed in-situ in two biomass-fired fluidised bed boilers (Henderson et al., 2015).

High-temperature corrosion in biomass fired boilers is still an insufficiently explored phenomenon which causes unscheduled plant shutdowns and hence, economic problems. To investigate the high-temperature corrosion and deposit formation behaviour of superheater tube bundles, online corrosion probe as well as deposit probe measurements have been carried out in a specially designed fixed bed/drop tube reactor to

simulate a superheater boiler tube under well-controlled conditions. The investigated boiler steel 13CrMo4-5 is commonly used as steel for superheater tube bundles in biomass fired boilers. Forest wood chips and quality sorted waste wood (A1-A2 according to German standards) as relevant fuels have been selected to investigate the influence on the deposit formation and corrosion behaviour. The following influencing parameter variations have been performed during the test campaigns: flue gas temperature between 650 and 880°C, steel temperature between 450 and 550°C and flue gas velocity between 2 and 8 m/s. One focus of the work presented is the detailed investigation of the structure and the chemical composition of the deposits formed as well as of the corrosion products. A further goal of the work presented was the development of an empirical model which can be used within CFD simulations of flow and heat transfer to calculate and evaluate the local corrosion potential of biomass fired plants already at the planning stage. The corrosion probe measurements show a clear dependency on the parameters investigated and the empirical function developed reproduces the measured corrosion behaviour sufficiently accurate. Since the additional calculation time within the CFD simulation is negligible the model represents a helpful tool for plant designers to estimate whether high-temperature corrosion is of relevance for a certain plant or not, when using fuels with similar compositions and the steel 13CrMo4-5 (Gruber et al., 2015).

Widely used CFD codes enable modelling of PC boilers operation one of the areas where these numerical simulations are especially promising is predicting deposition on heat transfer surfaces, mostly superheaters. The basic goal of all simulations is to determine trajectories of ash particles in the vicinity of superheater tubes. It results in finding where on the surface the tube will be hit by particles, and what diameter and mass flow of the particles are. This paper presents results of CFD simulations for a single tube and a bundle of in-line tubes as well. It has been shown that available parameters like ash particle density, shape factor, reflection coefficients affect the trajectories in a different way (Wacławiak et al., 2014). A steam-boost superheater was placed in that position and corrosion/deposit tests have been performed in part of the furnace within the less corrosive flue gas suggested by the CFD calculations. An air-cooled probe was used for exposures of the same material grades and temperatures as the permanently installed loop, but shorter exposure times in order to generate knowledge about the corrosion mechanisms and kinetics. Corrosion of superheater tubes is a serious problem during combustion of fuels with a high content of chlorine, such as waste and certain biomasses. The alkali chlorides are released to the flue gas and may condense on the heat exchanger tubes forming corrosive, chloride-rich deposits. In this work the effect of ammonium sulphate ((NH<sub>4</sub>)<sub>2</sub>SO<sub>4</sub>) injection on gaseous alkali chlorides, deposit chemistry and initial corrosion attack of superheater tubes during biomass combustion have been investigated (Viklund et al., 2015).

Higher steam temperatures can easily lead to higher corrosion rates of the superheaters due to aggressive species such as potassium chloride (KCl), which can be found in the deposits at the superheater surfaces. From the material point of view, corrosion can be reduced to a certain extent by modifying the chemical composition of superheater steels to enhance their resistance to corrosion. From the chemical point of view, the challenge can be approached by studying the corrosion reactions and mechanisms. Instead of preventing corrosion with expensive high-alloyed materials, possibilities such as oxide layer manipulation/passivation should be studied more thoroughly to find alternative and more cost-efficient ways to design materials with improved capability to resist corrosion (Lehmusto et al., 2015).

### 3. Experimental principles and methods

The first step is to cut the sample of pure titanium and TC4 alloy into 5 rectangular blocks respectively using a wire cutting machine and each was ground to 1000# with abrasive paper to have the same surface state. Then, these blocks are carefully cleaned with an ultrasonic cleaner and blown dry with a hair dryer. After that, the thickness of the sample is measured with a micrometer. The samples are then placed in a corrosive medium filled with the collected biomass superheater tube ash and the corrosive medium is placed in five crucibles respectively. The samples are divided into 5 groups and each group is equipped with a block of pure titanium and TC4 sample. Each group is put in a crucible respectively. The crucible is placed in a chamber electric resistance furnace and heated at a constant temperature to conduct the high temperature corrosion experiment. The corrosion temperature selected in the experiment is 550°C and 600°C because the corrosion rate of biomass superheater tube metal will have a significant increase above 550°C. The total time of the corrosion is 120 hours. Every 24 hours, a crucible is taken from the furnace to measure the degree of thinning. After the corrosion, the sample is taken from the crucible and the corrosive medium adhering to the sample is brushed off with a brush. After that, the XRD phase analysis will be conducted on the corrosion surface product. After the analysis, the corrosion samples are inlaid and sampled. The scanning electron microscope will be used to observe the end-face tissue of the oxide film after pre-grinding and polishing and the thickness of corrosion will be measured, obtaining the thinning of the sample.

## 4. Experimental Results and Analysis

### 4.1 Corrosion thinning degree and kinetic analysis

The kinetic equation of the heterogeneous reaction system at a constant temperature is:

$$\frac{d\alpha}{dt} = k(T)f(\alpha) \quad (1)$$

In this formula,  $\alpha$  is the conversion rate from reactants to products;  $t$  is time;  $f(\alpha)$  is the kinetic model function, which represents the reaction mechanism;  $K(T)$  is the reaction rate constant, which is commonly expressed by the Arrhenius formula, namely:

$$k(T) = A \exp\left(\frac{-E}{RT}\right) \quad (2)$$

In this formula,  $A$  is the pre-exponential factor;  $E$  is the activation energy;  $R$  is the universal gas constant;  $T$  is the thermodynamic temperature;  $X$  dynamic mode function integral form is as follows:

$$G(\alpha) = \int_0^\alpha \frac{d\alpha}{f(\alpha)} \quad (3)$$

When the corrosion temperature is 550°C, the experimental data of the comparison of pure titanium and TC4 alloy samples in corrosive medium of deposition ash in biomass superheaters is shown in Table and Table 2.

Table 1: Experimental results of TC4 sample 550 °C biomass superheater rotten media

	24h	48h	72h	96h	120h
Initial thickness	4.957	4.386	4.327	5.042	4.791
Thickness after etching	4.948	4.362	4.296	5.003	4.747
Thinning thickness	0.009	0.024	0.031	0.039	0.044

Table 2: Experimental results of pure Ti sample 550 °C biomass superheater rotten media

	24h	48h	72h	96h	120h
Initial thickness	4.952	4.379	4.336	5.023	4.782
Thickness after etching	4.941	4.353	4.301	4.974	4.711
Thinning thickness	0.011	0.026	0.035	0.049	0.071

The corrosive kinetic curve of pure titanium and TC4 alloy is shown in Figure 1.

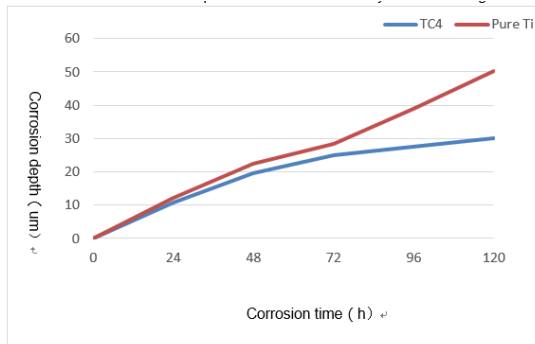


Figure 1: The corrosive kinetic curve of pure titanium and TC4 alloy

The corrosion thinning degree of pure Ti and TC4 samples at 600°C is larger than that at 550°C, which means that in the biomass corrosive medium, the corrosion degree of samples will increase with the temperature. The thinning degree of pure Ti samples is worse than that of TC4.

### 4.2 Analysis of corrosion products

With the increase of corrosion time, the corrosion degree of the surface of the TC4 alloy sample also increases. The surface of the passivation protective film cracks in the microscopic view, but it still maintain

good adhesion in the macroscopic view. Furthermore, the energy spectrum analysis of the surface morphology of the sample is conducted. The atomic percent of the element at the position 2 confirms with the elemental composition of the TC4 alloy, as is shown in Table 3, and the enrichment of the alkali metal element and the chlorine element is found at the position 1.

Table 3: Elemental analysis of corrosion of TC4 specimen

position	Atomic percentage of element							
	Ti	O	K	Ca	Cl	Al	V	C
1	48.16	30.56	0.51	0.54	0.68	12.39	7.00	0.15
2	85.18	-	-	-	-	9.47	4.88	0.47

The curves of pure titanium are slope-lined. That is, when the corrosion time increases, the corrosion of the base metal also increases; the corrosion kinetic curve of the TC4 alloy tends to be approximate parabola. That is, when the corrosion time increases, the corrosion of base tends to be flat, indicating that the oxide film of the pure titanium surface layer does not have protective effect on the substrate in the experimental simulation environment, while the oxide film of the TC4 alloy surface layer plays a certain protective role in the substrate. The corrosion degree of the two samples in the simulated biomass superheater corrosion medium is greater than that in the open air. In addition, with the increase of the experimental temperature, the corrosion degree of these two kinds of samples also increases and the corrosion degree of the pure titanium sample is more significant.

When conducting the line scanning the corrosion of pure titanium and TC4 alloy, the enrichment of Cl and K is found between the base metal and the corrosion layer and this phenomenon is more significant in the corrosion of pure titanium. The alkali metal and chlorine elements are engaged in the corrosion process. At high temperature, due to the strong diffusion and infiltration capacity of chlorine atoms, it can pass through the metal surface oxide film and react with the base metal to generate the corresponding metal chloride. The metal chlorides are volatile and its vapor pressure is high, thus creating pores in oxide film layer. Therefore, it increases the contacting opportunity between the active corrosive medium (alkaline molten salt, etc.) and the base metal. Moreover, the metal chloride will be oxidized to the corresponding metal oxides and chlorine close to areas with high oxygen partial pressure and the chlorine generated will return to the metal surface and continue to engage in the corrosion process.

It can be seen from the analysis of the comparison of the surface corrosion morphology and XRD of the two materials that the main phase of the surface corrosion layer of pure titanium is TiO<sub>2</sub> while the corrosion layer of TC4 alloy in the corrosive medium is the solid solution composite oxide formed by Al, V atom and TiO<sub>2</sub>. Due to the production of this composite oxide, the diffusion of alkali metal and chlorine elements in the corrosive medium is reduced, protecting the base metal.

#### 4.3 Impact of HCl Concentration

It can be seen from the change in KP of the pipe weight gain curve with the HCl concentration that the KP of 15CrMoG, 12Cr1MoVG, 12Cr2MoWVTIB and 20G increases significantly when the HCl concentration increases from 500 mL/m<sup>3</sup> to 2000 mL/m<sup>3</sup>, among which the increase of 20G is the most significant, as is shown in Table 4.

Table 4: Corrosion weight gain under 4 conditions for 4 pipes

Pipe	temperature	HCl concentration	K <sub>p</sub>
15CrMoG	500	2000	0.6310
	600	500	0.9069
12Cr1MoVG	500	2000	0.6452
	600	500	0.8780
12Cr1MoVG	500	2000	0.6000
	600	500	0.8058
20G	500	2000	1.0129
	600	500	1.0728

The vapor pressure of the metal chloride increases with the temperature. The higher vapor pressure indicates that the generated metal chloride can volatilize more quickly and diffuse to the oxide film, thereby promoting the reaction to accelerate towards the positive direction and the aggravating the corrosion. The increase in the

concentration of HCl in the reaction atmosphere pushes the reaction in the positive direction and generates more chlorine.

With the increase of temperature and HCl concentration, the T91 show significantly better anti-corrosion and heat resistance performance, which is related to their higher nickel content. It can be seen from Figure 2 that in the low oxygen partial pressure zone on the left side of the figure, when the partial pressure of chlorine rises to a certain critical value, the stable phase in the metal oxygen chlorine reaction system is converted from metal to metal chloride. The critical value of the partial pressure of chlorine corresponding to nickel is higher than that of titanium and chromium. That is, in the reaction of the metal/oxide interface with chlorine, the nickel is more stable than titanium and chromium. The above analysis indicates that nickel is the least reactive among titanium, chromium and nickel when reacted with chlorine.

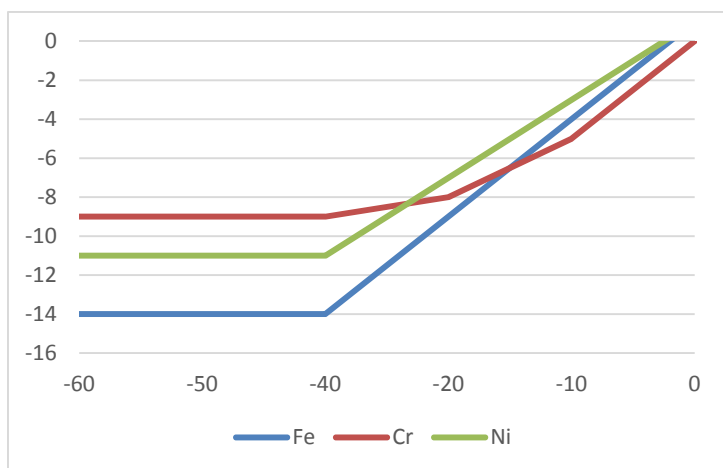


Figure 2: Thermodynamically stable phase diagram of a metal-oxygen-chlorine reaction system at 600°C

#### 4.4 Effect of cladding technology and compositional ratio on corrosion resistance

When the laser cladding is used for coating, due to the difference of coefficient of linear expansion between the base metal and the coating element, it is inevitable to cause internal stress, leading to cracks in the coating. Because there are many cracks in the pure titanium coating, the cracks are extended and expanded after the corrosion in the corrosive medium and reach the interface between the corrosion substrate and the coating. The corrosive medium, such as oxygen, enters into interior of the coating structure through the cracks, resulting in internal oxidation, thus increasing the corrosion of pure Ti coating sample. In the Ti-Al coating, cracks do not expand significantly and do not reach the substrate, thereby leading to no internal oxidation. In the Ti-Al-Mo coating, although the cracks reach the interface of the base metal, it does not cause serious internal oxidation. The coating samples adopting the two-story cladding coating had a smaller degree of oxidation and weight gain in the air medium and in the biomass corrosion medium than that in the one-story cladding coating, indicating that the multilayer cladding can improve the corrosion resistance of the coating. In addition, during the cladding process, the splashing of the hole and the base metal will affect the corrosion resistance of the coating, and the use of multilayer cladding process will reduce the occurrence of splashing of hole and base metal in the coating, so the impact of cladding process on the corrosion resistance of the coating is very significant.

In the air medium and biomass corrosive medium, the corrosion degree of pure titanium sample is the most significant, indicating that the corrosion resistance of pure titanium coating is worse than that of Ti-Al and Ti-Al-Mo coatings. The corrosion weight gain of Ti-Al coating is the smallest, followed by Ti-Al-Mo, which indicates that the Ti and Al elements in the coating selected for the experiment exert the most significant impact on the corrosion resistance of the coating. The energy spectrum analysis also verifies this point. The Ti and Al elements in the surface layer of the coating form an intermetallic compound with the Fe element in the base metal, together with the TiO<sub>2</sub> formed by the oxidation of the Ti element in the surface layer, constituting the composite oxide layer. Therefore, the high-temperature corrosion damage to the substrate is reduced and the corrosion resistance of the base is improved. In addition, through the observation of the coating structure after corrosion, it is found that the internal oxidation occurred in the structure due to the presence of cracks. However, Ti and Al elements are easier to oxidize than the Fe element in the base, so the oxidation occurs first in the coating. The expansion of cracks in the coating does not lead to significant oxidation inside the base metal.

## 5. Conclusion

In this paper, different kinds of tubes are selected for kinetic analysis, corrosion product analysis, HCl concentration effect analysis, etc. and the results show that the corrosion resistance of TC4 tube material is relatively good and the corrosion resistance of pure titanium tubes is relatively poorer compared with the former. In the experiment of the impact of HCl concentration, it is found that chemical reaction with chlorine. In China, there are relatively few researches on the superheater tubes in bio the tube with higher nickel content has better corrosion resistance, and the metal is the least likely to be engaged in the mass direct-fired boilers. Therefore, there may be deficiencies in the corrosion resistance experiment for superheater tube materials, which needs further studies.

## References

- Gruber T., Kai S., Scharler R. 2015, Investigation of the corrosion behaviour of 13CrMo4-5 for biomass fired boilers with coupled online corrosion and deposit probe measurements, *Fuel*, 144, 15-24, DOI: 10.1016/j.fuel.2014.11.071
- Henderson P., Szakálos P., Pettersson R. 2015, Reducing superheater corrosion in wood-fired boilers, *Materials & Corrosion*, 57(2), 128-134, DOI: 10.1002/maco.200503899
- Keiser J.R., Sharp W.B.A., Singbeil D.L. 2014, Could biomass-fueled boilers be operated at higher steam temperatures? Part 2: Field tests of candidate superheater alloys, *Tappi Journal*, 13(8), 51-63, DOI: 10.2172/1048711
- Lehmusto J., Yrjas P., Hupa M. 2015, The Effect of Pre-Oxidation on High-Temperature Corrosion Resistance of Superheater Steels, 25(3), 178-180, DOI: 10.4271/912298
- Okoro S.C., Kvisgaard M., Montgomery M. 2016, Pre-oxidation and its effect on reducing high-temperature corrosion of superheater tubes during biomass firing, *Surface Engineering*, 33(6), 428-432, DOI: 10.1007/s13632-016-0325-6.
- Stam A.F., Haasnoot K., Brem G. 2014, Superheater fouling in a BFB boiler firing wood-based fuel blends, *Fuel*, 135(11), 322-331, DOI: 10.1016/j.fuel.2014.06.030
- Viklund P., Kassman H., Åmand L. 2015, Deposit chemistry and initial corrosion during biomass combustion - The influence of excess O<sub>2</sub> and sulphate injection, *Materials & Corrosion*, 66(2), 118-127, DOI: 10.1002/maco.201307162.
- Wacławia k., Krzyszto F., Kalisz S. 2014, Influence of Selected Parameters on Ash Particle Trajectories When Modelling Deposition on Superheater Tubes in Pulverised Coal Boilers Using Fluent Code, *Chemical & Process Engineering*, 35(3), 305-316, DOI: 10.2478/cpe-2014-0023